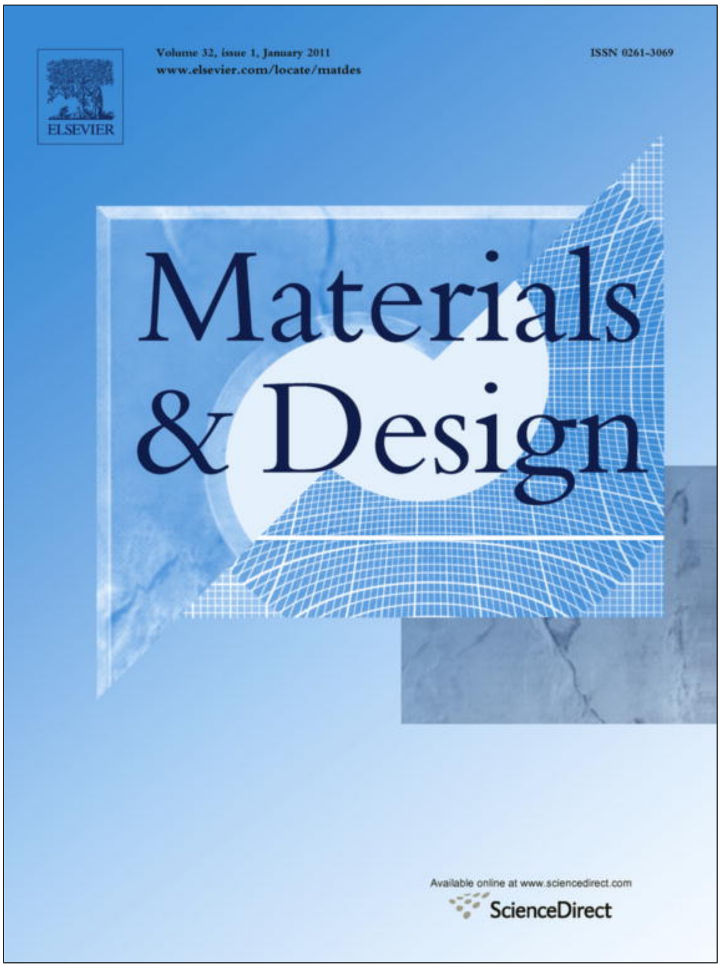

(This is a sample cover image for this issue. The actual cover is not yet available at this time.)

Materials and Design 34 (2012) 230–234

Contents lists available at SciVerse ScienceDirect

Materials and Design

journal homepage: www.elsevier.com/locate/matdes

Short Communication

Modeling of mechanical behavior of ultra fine grained aluminum produced by multiple compressions in a channel die

A. Rezaee-Bazzaz*, S. Ahmadian

Department of Metallurgy and Materials Engineering, Faculty of Engineering, Ferdowsi University of Mashhad, Mashhad, Iran

ARTICLE INFO

Article history:
Received 9 June 2011
Accepted 6 August 2011
Available online 12 August 2011

ABSTRACT

Mechanical behavior of AA1100 aluminum alloy processed by multiple compressions in a channel die was modeled on the basis of a generalized three-dimensional dislocation-density-based two-phase composite model. The simulated yield stress values were compared with the experimental data obtained by the multiple compressions in a channel die after several passes. A good agreement was found between the experimental and simulated yield stress values. The results showed that the yield stress of the ultra fine grained materials, produced by multiple compressions in a channel die, can reasonably be simulated using a dislocation-density-based two-phase model. Moreover, the experimentally determined average grain size of the studied material correlates well with that predicted by the model. Therefore, it can be said that the dislocation-based model could be used to predict the average grain size of the multiple compressed materials in a channel die.

1. Introduction

Severe plastic deformation (SPD) processing has been widely used for producing bulk ultra-fine grained materials, having grain sizes in the sub-micrometer or nanometer range [1–3]. Several SPD processing techniques, such as accumulative roll-bonding (ARB) [4], cyclic extrusion and compression (CEC) [5], multi-directional forging (MDF) [6], equal channel angular pressing (ECAP) [7], and high pressure torsion (HPT) [8] have been developed and successfully utilized for producing sub-micron materials. Among these SPD techniques, multi-directional forging, MDF, in which the specimen is subjected to uniaxial compression along three orthogonal axes to impart SPD, is conceptually very simple. However, since after pressing the lateral sides are barreled, the use of multiple compressions along different axes requires grinding of these surfaces before the next pressing can be carried out. The need for grinding after every pass could be reduced if the sample is pressed with a constraint on two of the four lateral sides, utilizing, for example, a channel die, usually used to simulate a plane strain rolling condition [9].

There exist few research reports about utilizing multi-directional forging and multiple compressions in a channel die as a means of imparting SPD [9–13]. Zherebstou et al. [12] investigated the production of sub-microcrystalline structure in a large scale Ti–6Al–4V billet by warm multi-directional forging. In their study, multi-directional forging was carried out at the temperature of 550 °C up to cumulative strain of three. A homogenous sub-microcrystalline structure with a grain/subgrain size of approximately 300 nm was reported. Kundu et al. [9] studied severe plastic deformation of copper using multiple compressions in a channel die. The results of their study revealed that a sub-microcrystalline structure could be produced after an equivalent strain of eight at ambient temperature. Multiple compressions in a channel die have been also attempted to severely deform an Al–Cu eutectic alloy [13], but failed because of fragmentation of the eutectic mixture. Microstructural evolution during multi-directional forging of copper showed that strain induced new grain structures develop as a result of the gradual increase in misorientation between subgrains [11].

Estrin et al. [14] proposed a two-dimensional dislocation cell structure model which has been recently generalized to three-dimensional states [15]. The model takes into account strain rate sensitivity and evolution of cell structure [16] and can predict the strain hardening of dislocation cell-forming materials during all stages of hardening; from stage II up to the end of stage V. There have been several attempts to predict stress–strain behavior and microstructure produced by some SPD processes by the use of the dislocation cell structure model. Mckenzie et al. [17] predicted the behavior of a wrought AA6016 alloy during ECAP up to 16 passes using a two-phase composite model, and showed that the model can predict the evolution of cell wall and cell interior dislocation densities very well. They also found that these parameters are functions of accumulated plastic strain as well as the level of hydrostatic pressure. Hosseini and Kazeminezhad [18–20] utilized the dislocation density based model for simulating the ECAP process and found that using this model, different microstructures

---

* Corresponding author. Tel.: +98 5118763305.
E-mail address: bazaz-r@um.ac.ir (A. Rezaee-Bazzaz).

0261-3069/$ - see front matter © 2011 Elsevier Ltd. All rights reserved.
doi:10.1016/j.matdes.2011.08.013

produced by ECAP with different die shapes can be predicted fairly well. They also investigated deformation behavior of Cu, Al and Ta through ECAP and showed that the dislocation density-based model can simulate the behavior of these materials well. The dislocation density-based model has also been applied to the case of HPT, where a good correlation between simulated and experimental microstructures was obtained [21]. It was claimed that a controversial issue of occurrence of uniform microstructure as a result of an inherently non uniform process was resolved.

The review of literature shows that although the dislocation density-based model has been used for modeling ECAP and HPT, there has been no attempt to simulate the multiple compressions in a channel die process using this approach. Since the main mechanisms of grain refinement in different SPD processes are almost the same, application of dislocation density-based model for simulating this process seems to be rational. The aim of this work is thus to show whether or not dislocation density-based model can be used for simulating yield stress of AA1100 aluminum alloy processed by multiple compressions in a channel die.

2. Model description

A three-dimensional version of the dislocation-density-based strain hardening model [14,15], which has been used in this study, is briefly reviewed for the sake of completeness. In this model, it is assumed that the material consists of two distinct but not independent phases; cell walls with dislocation density of ρ_w and cell interiors containing dislocations with lower density of ρ_i. The total dislocation density ρ_t is obtained by rule of mixtures:

$$\rho_t = f\rho_w + (1-f)\rho_i \tag{1}$$

where f is the volume fraction of cell walls. It has been reported that f decreases with strain, monotonically [22] and its evolution can be described by the following empirical equation [14]:

$$\frac{f-f_\infty}{f_0-f_\infty} = \exp\left(-\frac{\gamma^r}{\Omega}\right) \tag{2}$$

In the above equation f_0 is the initial value of f, f_∞ refers to the saturation value of f at large strains and Ω shows the rate of variation of f with respect to shear strain, γ^r.

The average cell size, d, is inversely related to the total dislocation density by:

$$d = \frac{K}{\sqrt{\rho_t}} \tag{3}$$

where K is the cell size factor and decreases by increasing the accumulated shear strain, similar to cell wall volume fraction variation:

$$\frac{K-K_\infty}{K_0-K_\infty} = \exp\left(-\frac{\gamma^r}{\Gamma}\right) \tag{4}$$

where K_0, K_∞ and Γ are numerical constants.

The evolution of the dislocation density in cell interiors and cell walls is governed by the following equations, respectively [14].

$$\dot{\rho}_i = \frac{\alpha^*}{\sqrt{3}}\frac{\sqrt{\rho_w}}{b}\dot{\gamma}_w - \frac{6\beta^*\dot{\gamma}_i}{bd(1-f)^{1/3}} - R_i\left(\frac{\dot{\gamma}_i}{\dot{\gamma}_0}\right)^{-1/n_i}\dot{\gamma}_i\rho_i \tag{5}$$

$$\dot{\rho}_w = \frac{6\beta^*\dot{\gamma}_i(1-f)^{2/3}}{bdf} + \frac{\sqrt{3}\beta^*\dot{\gamma}_i(1-f)\sqrt{\rho_w}}{fb} - R_w\left(\frac{\dot{\gamma}_w}{\dot{\gamma}_0}\right)^{-1/n_w}\dot{\gamma}_w\rho_w \tag{6}$$

The first term in the right hand side of Eq. (5) shows the rate of dislocation generation in cell interiors by the Frank–Read mechanism. The second term represents the loss rate of cell interior dislocations by moving into the walls and becoming part of wall structure and the last term describes the annihilation rate of dislocations in the cell interior by dynamic recovery. The geometry parameters, α^* and β^* are considered to be constants, and R_i, n_i, $\dot{\gamma}_i$, $\dot{\gamma}_w$ and $\dot{\gamma}_0$ are the recovery factor in the cell interior, recovery exponent in the cell interior, shear strain rate in the cell interior, shear strain rate in cell walls and reference shear strain rate, respectively. The first term in the right hand side of Eq. (6) represents the dislocation density gain in the walls caused by the loss of dislocations in cell interiors. The second term expresses the increase of dislocation densities in the walls by activation of the Frank–Read sources at the interface by dislocations coming from cell interiors, and the third term accounts for the annihilation of cell wall dislocations by dynamic recovery at high strains. R_w and n_w are the recovery factor and recovery exponent in cell walls, respectively. To satisfy strain compatibility along the interface between cell interiors and cell walls, the following relation is imposed [15]:

$$\dot{\gamma}_i = \dot{\gamma}_w = \dot{\gamma}^r \tag{7}$$

Solving Eqs. (5) and (6) simultaneously by numerical methods, dislocation densities in both cell interiors and cell walls are computed. Using Eq. (1), the total dislocation density can also be calculated. The yield stress of the studied polycrystalline material is obtained based on the following equation:

$$\sigma_y = \sigma_0 + \alpha MGb\sqrt{\rho_t} \tag{8}$$

where σ_0 is the lattice friction stress at a constant temperature, G is the shear modulus, α is a numerical constant, and M is the Taylor factor. The present model is also able to predict the average cell size of the material by using Eq. (3).

3. Experimental procedure

3.1. Material and processing

The material used were commercially pure aluminum (AA1100) blocks, the chemical composition of which is shown in Table 1. From these blocks, samples with dimensions 7.5 mm × 14.8 mm × 15 mm were cut and used for the subsequent processing. The specimens were fully annealed at 673 K for 1 h to eliminate any effect of previous thermomechanical history. Usual metallographic procedures revealed that the mean grain size of the specimens after annealing was about 33 μm.

The annealed specimens were compressed several times in a channel die. The pressings were carried out at room temperature using a ram speed of 25 mm s^{-1} and mineral oil used as lubricant. A specimen of height 15 mm and 14.8×7.5 mm^2 section was placed in the die in such a way that the 14.8 mm side just slides into the 15 mm wide channel. Fig. 1 shows the deformation scheme during multiple compressions in a channel die. The sides of the specimen are designated as A, B and C. The first pressing was carried out on face A to half of the height of the sample. This makes the side which was previously 7.5 mm to be about 14.8 mm. The specimen is then rotated such that the second pressing was carried out on face B. The 14.8 mm side slides into 15 mm wide channel and the side that was previously 15 mm, becomes the height for the next pressing. After the second pressing, the specimen was rotated such that the next pressing was carried

Table 1
Chemical composition of the AA1100 aluminum alloy.

Al	Si	Fe	Cu	Mn	Mg	Zn	Ti	Ni	Ca
Bal.	0.171	0.345	0.055	0.009	0.006	0.025	0.005	0.002	0.011

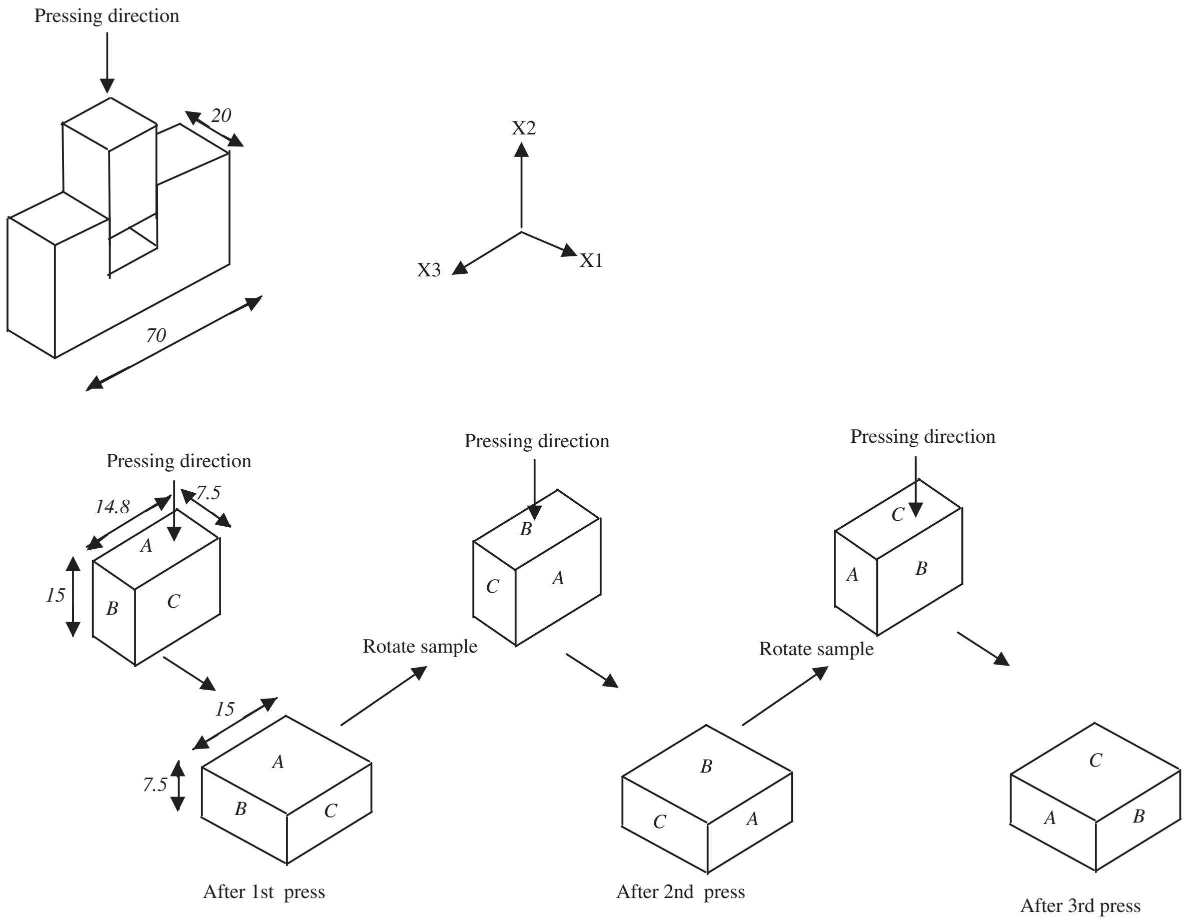

Fig. 1. Schematic illustration of the sequence of multiple compressions in a channel die process [9].

out on face C. After each pressing, the specimen was rotated and reinserted into the channel such that the specimen dimension equal to the channel width becomes the height for the next pressing. This sequence ensures that the sample is pressed in all three directions. It is worth noting that after each pressing pass, the grinding carried out on the bulged portion of the sample to preserve its initial dimensions. The above mentioned stages were repeated up to eight passes ($\varepsilon = 6.4$).

3.2. Mechanical testing

Uniaxial compression specimens, 10 mm in height and 5.64 mm in diameter, were machined from the processed specimens. Compression tests were carried out at ambient temperature using a screw driven Zwick Z250 universal testing machine at a constant cross head speed of 1.2 mm min^{-1}, corresponding to an initial strain rate of $2 \times 10^{-3}\ \text{s}^{-1}$

Microhardness of the processed specimens was measured by a Buhler microhardness testing machine using the Vickers indenter under applied load of 25 g. Each reported hardness was an average of at least five separate measurements taken at random places on the surface of the specimen. All the indentations were at least 5 mm away from the edges and from other indentations.

3.3. TEM observations

The microstructural observation by transmission electron microscopy (TEM) was done for the specimens after multiple compressions in the channel die. To prepare TEM thin foils, specimens were ground to a thickness of about 100 μm and then electropolished by a twin-jet, using a 33% HNO_3 and 66% CH_3OH solution at −30 °C and 20 V. Leo 912 transmission electron microscope operated at 120 kV was used for microstructural examination.

4. Results and discussion

Fig. 2a and b shows the respective variations of yield stress and microhardness with respect to the number of pressing passes. According to Fig. 2a, the yield strength of the studied material increases with increasing the imposed strain. The maximum strength gain occurs after the first pass of the process. Yield stress of the multiple compressed material in a channel die changes from 68 MPa at the start of the process to 264 MPa after eight passes. This is approximately 3.9 times greater than the yield stress of the material at the start of the process. Similar changes in yield strength have been already reported for the same material processed by the ARB method [23,24]. According to Fig. 2b, the trend of microhardness changes of the studied material with respect to the pressing passes is similar to the trend of yield strength changes with compression cycles. This fact shows that there exist a correlation between yield stress and microhardness in the multiple compressed materials in a channel die similar to those usually observed in the conventionally processed materials.

As mentioned earlier, in the dislocation-density-based model, the material is assumed to be composed of cell interiors and cell walls. According to the published reports, aluminum is a dislocation cell-forming material and the size of the dislocation cells depends on the dislocation density [18,23–25]. All of the model parameters and constants which are necessary for application of this model to multiple compressions of aluminum in a channel

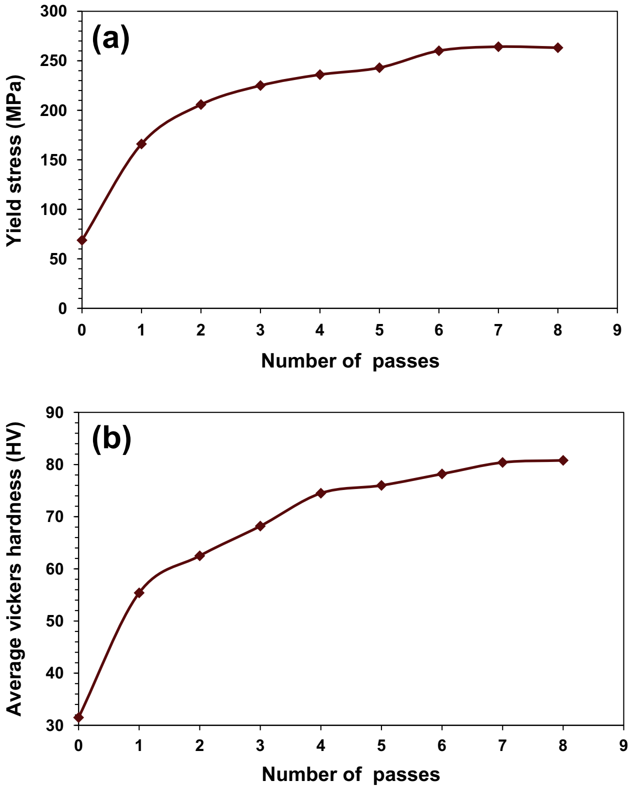

Fig. 2. (a) Variations of yield stress, and (b) microhardness with number of passes of multiple compressions in a channel die.

Table 2
The values of parameters and constants used in the model [16–19].

α^*	0.0024
β^*	0.0054
k_i	13
k_∞	6.5
α	0.25
M	3.06
G (MPa)	26.3×10^3
f_0	0.25
f_∞	0.06
Ω	2.11
$\dot{\gamma}_0^r(s^{-1})$	1
$\rho_i^{r=0}(m^{-2})$	10^{13}
$\rho_w^{r=0}(m^{-2})$	10^{14}
Γ	3.85
R_i	11.5
R_w	6.9
n_i	67
n_w	4
$b(m)$	2.86×10^{-10}

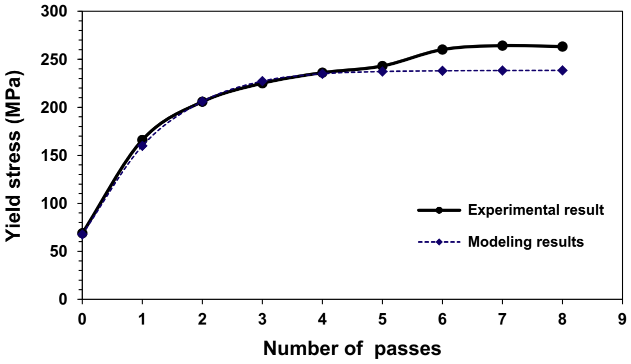

Fig. 3. Variation of yield stress with accumulated strain.

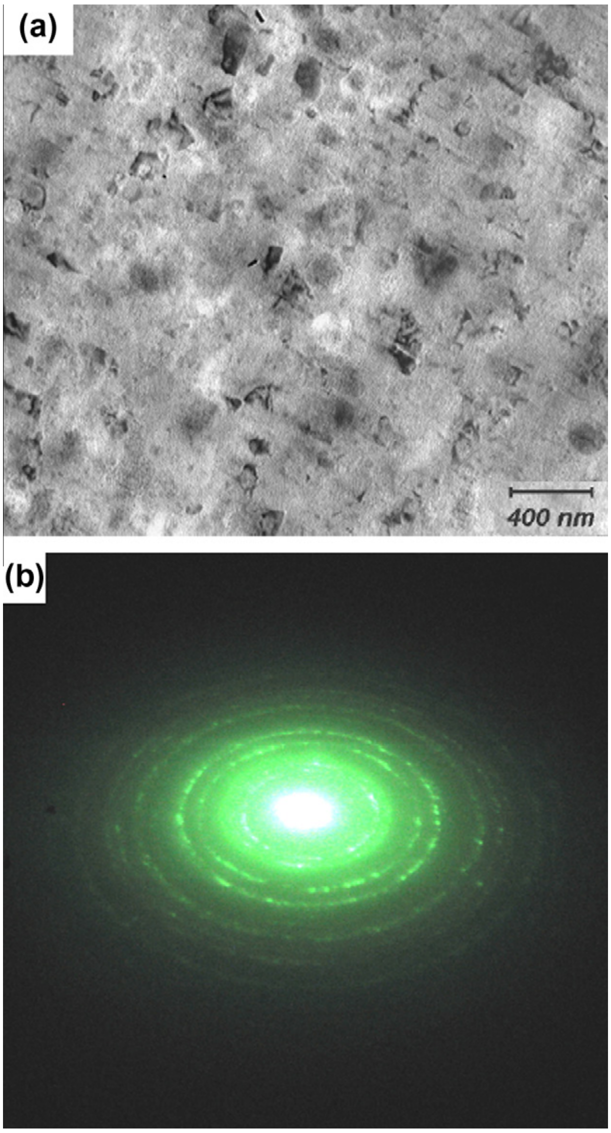

Fig. 4. TEM micrographs and the corresponding SAD pattern of commercially pure aluminum after eight passes of multiple compressions in a channel die.

die are summarized in Table 2. The results of dislocation-density-based model for predicting the variation of yield stress with accumulated strain are illustrated in Fig. 3. For comparing the predicted results with experimentally determined yield stresses, the variation of the experimentally obtained yield stress with accumulated strain was superimposed in Fig. 3. It is clear from the figure that the difference between the calculated and measured yield stress values becomes greater in the last three passes than that of previous ones. Thus, it can be said that the accuracy of the model predictions at high accumulated strains decreases. Comparison of the experimental yield stress variations versus accumulated strain with predicted ones shows that the maximum difference between experimental and predicted results is about 7%. Therefore, it can be concluded that the dislocation-based model can predict yield stress variations with accumulated strain with a good accuracy.

Fig. 4a and b shows the TEM microstructure of the studied material after eight pressing passes together with the

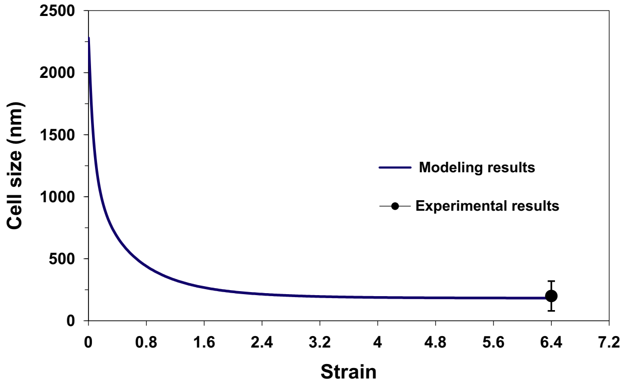

Fig. 5. Change of cell size as a function of accumulated strain.

corresponding selected area diffraction pattern, respectively. It is clear that ultrafine grains are produced after eight passes of the process. The mean grain size of the material was measured using linear intercept method and it was found that eight cycles of multiple compressions in a channel die produces the ultrafine grain material with grain sizes in the range of 80–200 nm. The ring pattern of SAD is an evidence for the existence of fine grains with high angle boundaries. Such a microstructure is similar to that reported for the same material processed by the accumulative roll-bonding [24–26].

In the application of the model to the multiple compressions in a channel die in the present study, it is tacitly assumed that a new refined grain structure emerges as the misorientation between cell structure increases with strain. The cell structure can thus be considered as grain structure, similar to the assumptions made in application of the model to ECAP and HPT [17,21,27], and according to the experimental findings in muli-directional forging of copper [11]. Therefore, in this modeling approach, the theoretically calculated average cell size is assumed to be the average grain size which was calculated by the model. This can be compared with the experimentally determined average grain size. Changes of the cell size as a function of accumulated strain predicted by the dislocation-density-based model obtained in this study is shown in Fig. 5. As the figure shows, the maximum drop in the average cell size occurs after the first pass of the process, the same as that reported in the ARB process [24]. Due to the lack of experimental data, only the average grain size obtained in this work after eight pressing passes was superimposed on the figure. As it is clear from the figure, the experimentally determined average grain size after eight pressing passes which corresponds to accumulated strain of 6.4, correlates well with predictions of the model. Therefore, it can be concluded that dislocation-based model could be used to predict the average grain size of the multiple compressed materials in a channel die.

5. Conclusions

An existing two-phase composite model based on dislocation density evolution was used to predict the variation of yield strength of AA1100 aluminum alloy during multiple compression passes in a channel die. Comparison of the predictions with experimental results revealed that there is a good agreement between model predictions and experimental findings. Moreover, using this model, the mean grain size of the studied material after eight pressing passes was predicted and compared with the average grain size obtained experimentally. The agreement between predictions and experimental results was excellent. In summary, the variation of the yield strength of AA1100 aluminum alloy by multiple compression passes in a channel die can satisfactorily be predicted and the average grain size of the studied multiple compressed material in a channel die could be estimated by the use of a simple composite dislocation-based model.

References

[1] Valiev RZ, Islamgaliev RK, Alexandrov IV. Bulk nanostructured materials from sever plastic deformation. Prog Mat Sci 2000:103–89.
[2] Valiev RZ. Nanostructuring of metals by sever plastic deformation for advanced properties. Nat Mater 2004;3:511–6.
[3] Valiev RZ, Estrin Y, Horita Z, Langdon TG, Zehetbauer MJ, Zhu YT. Producing bulk ultrafine-grained materials by sever plastic deformation. JOM 2006;58:33–9.
[4] Saito Y, Utsunomiya H, Tsuji N, Sakai T. Novel ultra-high straining process for bulk materials development of the accumulative roll-bonding (ARB) process. Acta Mater 1999;47:579–83.
[5] Richert J, Richert M. A new method for unlimited deformation of metals and alloys. Aluminium 1986;62:604–7.
[6] Salishchev GA, Valiahmetov OR, Galeev RM. Formation of submicrocrystalline structure in titanium alloy VT8 and its influence on mechanical properties. J Mater Sci 1993;28:2898–902.
[7] Valiev RZ, Krasilinkov NA, Tsenev NK. Plastic deformation of alloys with submicron-grained structure. Mater Sci Eng A 1991;137:35–40.
[8] Horita Z, Smith DJ, Furukawa M, Nemoto M, Valiev RZ, Langdon TG. Evolution of grain boundary structure in submicrometer-grained Al–Mg alloy. Mater Charact 1996;35:285–94.
[9] Kundu A, Kapoor R, Tewari R, Chakravartty JK. Severe plastic deformation of copper using multiple compression in a channel die. Scr Mater 2008;58:235–8.
[10] Vorhauer A, Pippen R. The influence of type and path of deformation on the microstructural evolution during severe plastic deformation. In: Zehtbauer M, Valiev RZ, editors. Nanomaterials by severe plastic deformation. Weinheim: Wiley VCH; 2004. p. 684–90.
[11] Belyakov A, Sakai T, Miura H, Tsuzaki K. Grain refinement in copper under large strain deformation. Philos Mag 2001;81:26–9.
[12] Zherebstou SV, Salishchev GA, Galeyev RM, Valiakhmetov OR, Mironov SY, Semiatin SL. Production of submicrocrystalline structure in large-scale Ti–6Al–4V billet by warm severe deformation processing. Scr Mater 2004;51:1147–51.
[13] Parimi AK, Robi PS, Dwivedy SK. Severe plastic deformation of copper and Al–Cu alloy using multiple channel-die compression. Mater Des 2011;32:1948–56.
[14] Estrin Y, Toth LS, Molinari A, Brechet Y. A dislocation based model for all hardening stages in large strain deformation. Acta Mater 1998;46:5509–22.
[15] Toth LS, Molinari A, Estrin Y. Strain hardening at large strains as predicted by dislocation based polycrystal plasticity model. Eng Mater Technol 2002;124:71–7.
[16] Enikeev NA, Kimb HS, Alexandrov IV. Kinetic dislocation model of microstructure evolution during severe plastic deformation. Mater Sci Eng A 2007;460(461):619–23.
[17] Mckenzie PWJ, Lapovok R, Estrin Y. The influence of back pressure on ECAP processed AA6016: modeling and experiment. Acta Mater 2007;35:2985–93.
[18] Hosseini E, Kazeminezhad M. The effect of ECAP die shape on nanostructure of materials. Comput Mater Sci 2009;44:962–7.
[19] Hosseini E, Kazeminezhad M. A hybrid method on severe plastic deformation of copper. Comput Mater Sci 2009;44:1107–15.
[20] Hossini E, Kazeminezhad M. Dislocation structure and strength evolution of heavily deformed tantalum. Int J Refract Met Hard Mater 2009;27:605–10.
[21] Estrin Y, Molotnikov A, Davies CHJ, Lapovok R. Strain gradient plasticity modeling of high-pressure torsion. J Mech Phys Solids 2008;56:1186–202.
[22] Muller M, Zehetbauer M, Borbely A, Ungar T. Stage IV work hardening in cell forming materials, part I: features of the dislocation structure determined by X-ray line broadening. Scr Mater 1996;35:1461–6.
[23] Pirgazi H, Akbarzadeh A, Petrov R, Kestens L. Microstructure evolution and mechanical properties of AA1100 aluminum sheet processed by accumulative roll-bonding. Mater Sci Eng A 2008;497:132–8.
[24] Rezaee-Bazzaz A, Ahmadian S, Reihani H. Modeling of microstructure and mechanical behavior of ultrafine grained aluminum produced by accumulative roll-bonding. Mater Des 2011;32:4580–5.
[25] Winther G, Huang X, Godfery A, Hansen N. Critical comparison of dislocation boundary alignment studied by TEM and EBSD: technical issue and theoretical consequences. Acta Mater 2004;52:4437–46.
[26] Ezadjou M, Daneshmanesh H, Janghorban K. Microstructural and mechanical properties of ultra-fine grains (UFG) aluminum strips produced by ARB process. J Alloy Compd 2009;474:406–15.
[27] Baik SC, Estrin Y, Kim Hs, Helming RJ. Dislocation density based modeling of deformation behavior of aluminum under equal channel angular pressing. Mater Sci Eng A 2003;351:86–97.